

# SPEEK/epoxy resin composite membranes *in situ* polymerization for direct methanol fuel cell usages

Tiezu Fu, Chengji Zhao, Shuangling Zhong,  
Gang Zhang, Ke Shao, Haiqiu Zhang, Jing Wang, Hui Na\*

Alan G. MacDiarmid Institute, College of Chemistry, Jilin University, Qianwei Road 2699#, Changchun 130012, PR China

Received 31 October 2006; received in revised form 7 December 2006; accepted 11 December 2006

Available online 22 December 2006

## Abstract

Sulfonated poly(ether ether ketone) (SPEEK)/4,4'-diglycidyl(3,3',5,5'-tetramethylbiphenyl) epoxy resin (TMBP) composite membranes *in situ* polymerization were prepared for the purpose of improving the methanol resistance and mechanical properties of SPEEK membranes with high ion-exchange capacities (IEC) for the usage in the direct methanol fuel cells (DMFCs). The effects of introduction of TMBP content on the properties of the composite membranes were investigated in detail. The composite membranes have good mechanical, thermal properties, lower swelling ratio, lower water diffusion coefficient ( $0.87 \times 10^{-5} \text{ cm}^2 \text{ s}^{-1}$  at  $80^\circ\text{C}$ ) and better methanol resistance ( $5.26 \times 10^{-7} \text{ cm}^2 \text{ s}^{-1}$  at  $25^\circ\text{C}$ ) than SPEEK membranes. The methanol diffusion coefficients of the composite membranes are much lower than that of SPEEK membrane ( $17.5 \times 10^{-7} \text{ cm}^2 \text{ s}^{-1}$  at  $25^\circ\text{C}$ ). Higher selectivity was been found for the composite membranes in comparison with SPEEK. Therefore, the SPEEK/TMBP composite membranes show a good potential in DMFCs usages.

© 2007 Elsevier B.V. All rights reserved.

**Keywords:** SPEEK; TMBP; Composite membrane; DMFCs

## 1. Introduction

The proton exchange membrane fuel cells (PEMFCs), especially direct methanol fuel cells (DMFCs) are a type of fuel cell, which are promising clean power sources for vehicular transportation, residential and industrial, and also for computers and mobile communication equipment because of the simple fuel cell setup (easy storage of methanol, no reformer required), low emissions and low operating temperatures [1–3]. Proton exchange membranes (PEMs) are one of the most important components of the proton exchange membrane fuel cell because they provide ionic pathways for protons and prevent cross-over of gases in fuel cells. So far only a few membrane types have been used as the proton conductor in DMFCs such as Dupont Nafion®. They show good performance such as their excellent chemical and mechanical stabilities as well as high proton conductivity in fuel cells. However, the high cost, low conductivity at high temperature and high methanol permeability of Nafion®

limited their usages. For this reason, many researchers hope to develop high performance, low cost and high proton conductive electrolyte membranes.

Recently many efforts have been devoted to developing new materials for proton exchange membranes based on sulfonated aromatic polymers, such as poly(aryl ether ketone)s [4–7], poly(ether sulfone)s [8,9], polyimides [10,11]. These copolymers are satisfied with lower cost as well as chemical stability for many applications.

Poly(aryl ether ketones) (PAEKs) are high-performance engineering thermoplastics for the excellent mechanical properties, high thermal stability, resistance to oxidation and stability under acidic conditions. Thus, sulfonated PAEKs have been development as alternative PEM materials [12–15]. However, the sulfonated PAEKs with high ion-exchange capacities (IEC) have relatively high methanol permeability, high swelling ratio and low mechanical properties at evaluated temperatures, which limit them the available usage in applications on DMFCs, although they exhibit high proton conductivity [9,10,12–16]. For solving these problems, acid–base composite membranes have been widely studied, recently. Kerres and co-workers [17,18] and Han and co-workers [19] have investigated the blend of

\* Corresponding author. Tel.: +86 431 85168870; fax: +86 431 85168868.  
E-mail address: [huina@jlu.edu.cn](mailto:huina@jlu.edu.cn) (H. Na).

the SPEEK with amine group polymers due to the formation of hydrogen bond between the sulfonic acid groups and amine groups. The hydrogen bond will lead to the compatibility of the blend polymers. This will be in favor of swelling reduction, improvement of mechanical property and further decreasing the methanol cross-over of membranes [17,18]. Blending with amine polymers also will lead to the protons transfer from protonated-amine groups to the sulfonic groups of the blend polymers [19]. In our previous study [20,21], the PANI and PPy with amine groups have been added into the SPAEKs to form acid–base composite membranes. As the reported, the composite membranes have overcome the above drawbacks.

Epoxy resins have been widely used as high performance materials in many fields, such as adhesive, coating, laminating capsulation, electrical insulation, and composite applications [22–25]. The epoxy resins have exhibited good thermal properties, chemical resistance and electric insulation through a cross-linking reaction with a curing agent to make the three-dimensional network structure. Recently, epoxy resins containing rigid rod structure have been synthesized as a new class of high performance polymers [26–28]. A rigid rod material typically has a rigid rod segment in the polymer chain either on the polymer backbone or on the side chain. Rigid rod epoxy resins have been developed as a high performance polymer for electronic and aerospace applications due to their good thermal stability and unique physical properties. Rigid rod epoxy resins in particular potentially enhanced thermal stability and dielectric properties over conventional epoxy resin [29–32]. Polyamide (PA) with amine groups was selected as curing agent for epoxy resin because of the possibility of forming the hydrogen bonds between the sulfonic acid groups in SPEEK matrix and amine groups in PA.

In this paper, we reported a new composite membrane with *in situ* polymerization between TMBP and PA in SPEEK membrane. The effects of introduction of epoxy resin into SPEEK

membranes with high IEC on the mechanical properties, water uptake, swelling ratio, proton conductivity and methanol permeability were investigated to evaluate their potential applications for DMFCs.

## 2. Experiment

### 2.1. Materials

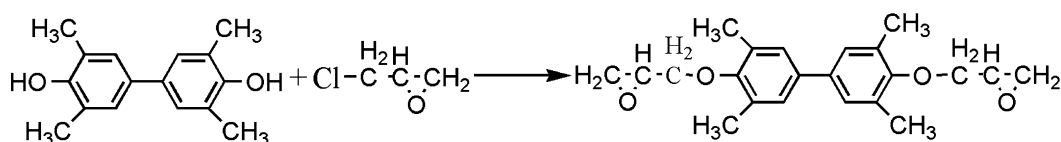
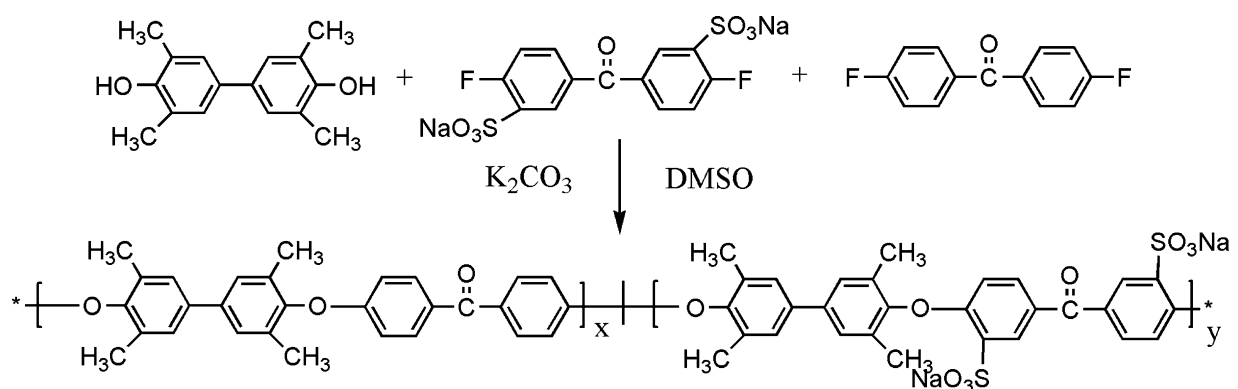
Sulfonated poly(ether ether ketone) was prepared by direct aromatic nucleophilic substitution step polymerization. Detailed synthesis procedures and characterization of this copolymer were described in a previous article [12].

The epoxy monomer, 4,4'-diglycidyl(3,3',5,5'-tetramethylbiphenyl)epoxy resin (TMBP) with the epoxy equivalent of 177 used in this study was synthesized according to our previously reported procedure [33–35]. Polyamide (PA) (trade name 650<sup>#</sup>) with small molecular weight used as curing agent was purchased from Beijing Chemical Works, China.

The preparation and the chemical structure of sulfonated poly(ether ether ketone) (SPEEK) and 4,4'-diglycidyl(3,3',5,5'-tetramethylbiphenyl)epoxy resin (TMBP) were shown in Scheme 1.

### 2.2. Preparation of composite membranes

The SPEEK and the SPEEK/TMBP composite membranes were prepared by solution casting and evaporation method. The SPEEK was dissolved in DMF at room temperature to prepare a 10 wt% solution. The requisite quantity of TMBP and PA monomers (TMBP/PA = 4/3 (w/w)) was added to the polymer solution and stirred for about 3 h and then cast onto a glass plate. The membranes (50–150  $\mu\text{m}$ ) were dried at 85  $^{\circ}\text{C}$  for 10 h and dried in a vacuum oven at 100  $^{\circ}\text{C}$  for 48 h, then heated at 180  $^{\circ}\text{C}$  for 1 h for thermal activation of the cross-linking reac-



Scheme 1. The preparation and the chemical structure of SPEEK and TMBP.

tion between TMBP and PA. Each membrane on the glass plate was peeled off from the glass plate by immersing them in deionized water. The membranes in acidic form were obtained by immersing into a 2 M HCl solution for 24 h, and then the membranes were washed with deionized water until the pH reached 6–7. In the following sections, composite membranes having different weight percentages of TMBP and PA will be referred as SPEEK/TMBPX, where ‘X’ represents weight percentages of TMBP and PA, and TMBP cured by PA will be referred as TMBP for short.

### 2.3. The characterization of the composite membranes

The FTIR spectroscopy of dry membrane samples was recorded on the power samples dispersed in dry KBr in form of disks, using a BRUKER Vector 22 spectrometer at a resolution of  $4 \text{ cm}^{-1} \text{ min}^{-1}$  from 4000 to  $400 \text{ cm}^{-1}$ .

UV–vis spectra were performed on UV-2501 PC Spectrometer (SHTMADU, Tokyo, Japan) with the membranes.

The morphologies of SPEEK/TMBP composite membranes were determined by atomic force microscopy (AFM). AFM is performed with SHIMADZU SPM-9500 JZ Scanning Probe Microscope, Japan in tapping mode. A silicon microcantilever (spring constant  $2 \text{ N m}^{-1}$  and resonance frequency  $\sim 70 \text{ kHz}$  Olympus Co., Japan) with an etched conical tip (radius of curvature  $\sim 40 \text{ nm}$  as characterized by scanning over very sharp needle array, NT-MDT, Russia) is used for scan. The scan rate ranged from 1.0 to 2.0 Hz to optimize the image quality. Each scan line contains 256 pixels, and a whole image is composed of 256 scan lines. The SPEEK/TMBP membranes were obtained by spin-coating a solution of SPEEK, TMBP and PA in  $0.05 \text{ g ml}^{-1}$  DMF on freshly cleaned silicon wafer at 3000 rpm for 40 s at room temperature, and then heating at  $180^\circ \text{C}$  for 1 h.

The tensile strength of the membranes was measured using SHIMADZU AG-I 1KN at the test speed of  $2 \text{ mm min}^{-1}$ . The size of specimen is  $15 \text{ mm} \times 4 \text{ mm}$ . For each testing reported, at least three specimens were measured and average value was calculated.

A METTLER 821<sup>c</sup> model DSC was employed to determine the glass transition temperature ( $T_g$ ) of the membranes. The samples were preheated over a temperature range of  $25\text{--}350^\circ \text{C}$  at a heating rate of  $10^\circ \text{C min}^{-1}$  under  $\text{N}_2$  with the flow of  $200 \text{ ml min}^{-1}$  to remove moisture for avoiding the effects of the thermal history, then cooled to  $25^\circ \text{C}$  and reheated from 25 to  $350^\circ \text{C}$  at a heating rate of  $10^\circ \text{C min}^{-1}$ .

A Pyris TGA (Perkin-Elmer) was used to study the thermal stability behaviors of the membranes. About 5–10 mg samples of the membranes were heated to  $150^\circ \text{C}$  and kept at this temperature for 20 min to remove any residual water and solvents then cooled to  $80^\circ \text{C}$  and reheated to  $700^\circ \text{C}$  at a heating rate of  $10^\circ \text{C min}^{-1}$  under a nitrogen atmosphere.

The water uptake of the membranes at different temperatures was calculated by measuring the weight difference between the dry and swollen membranes as follow [10,12,16]: the membranes were first equilibrated in water at a given temperature for about 12 h, then removed from water quickly, blotted the membrane surface to remove any excess water with filter paper, and

immediately weighed the wet mass ( $W_{\text{wet}}$ ) and thick ( $T_{\text{wet}}$ ). The membranes were then dried at  $120^\circ \text{C}$  for 24 h. The dried weight ( $W_{\text{dry}}$ ) and thick ( $T_{\text{dry}}$ ) of membranes was measured. The water uptake was calculated by the following equation:

$$\text{water uptake (WU) (\%)} = \frac{W_{\text{wet}} - W_{\text{dry}}}{W_{\text{dry}}} \times 100 \quad (1)$$

The swelling ratio was defined as follows:

$$\text{swelling ratio (\%)} = \frac{T_{\text{wet}} - T_{\text{dry}}}{T_{\text{dry}}} \times 100 \quad (2)$$

The number of water molecules per sulfonic site ( $\lambda$ ) can be determined by the following equation:

$$\lambda = \frac{(W_{\text{wet}} - W_{\text{dry}})/M_{\text{H}_2\text{O}}}{W_{\text{dry}} \text{IEC}} \quad (3)$$

The classical titration method was used to determine the IEC of the membranes [36]. Firstly, the membranes in the acid form ( $\text{H}^+$ ) were converted to the sodium form by immersing the membranes in a 1 M NaCl solution for 24 h to exchange the  $\text{H}^+$  ions with  $\text{Na}^+$  ions. Then, the exchanged  $\text{H}^+$  ions within the solutions were titrated with a 0.01 M NaOH solution.

The titrated IEC was determined from the following equation:

$$\text{IEC (mequiv./g)} = \frac{\text{consumed ml NaOH} \times \text{molarity NaOH}}{\text{weighty dried membrane}} \quad (4)$$

For each sample, at least three measurements were carried out until the values had little derivation.

The water desorption measurement was made by Pyris 1 TGA (Perkin-Elmer), which was used to determine the weight changes of samples with time at  $80^\circ \text{C}$ . Water diffusion coefficient is calculated as follows [37]:

$$\frac{M_t}{M_\infty} = 4 \left( \frac{D_t}{\pi l^2} \right)^{1/2} \quad (5)$$

where  $D$  is the water diffusion coefficient,  $M_t/M_\infty$  the water desorption, and  $l$  is the membrane thickness.

Methanol diffusion coefficients of membranes were measured by using a two-chamber liquid permeability cell described in the literature [12,18,38] as shown in Fig. 1. This cell consisted of two reservoirs, which were separated by a vertical membrane immersed in deionized water for 24 h. Ten molar methanol solutions were placed on one side of the cell and water was placed on the other side. The magnetic stirrers were used continuously during the measurement. Methanol concentrations in the water cell were periodically determined by using a GC-8A gas chromatograph (SHTMADU, Tokyo, Japan). The methanol diffusion coefficient was calculated in equation:

$$C_B(t) = \frac{A}{V_B} \frac{DK}{L} C_A(t - t_0) \quad (6)$$

where  $A$ ,  $L$  and  $V_B$  were the effective area, the thickness of membrane and the volume of permeated reservoirs, respectively.  $C_A$  and  $C_B$  were the methanol concentration in methanol chamber and water chamber, respectively.  $DK$  was the methanol diffusion coefficient.

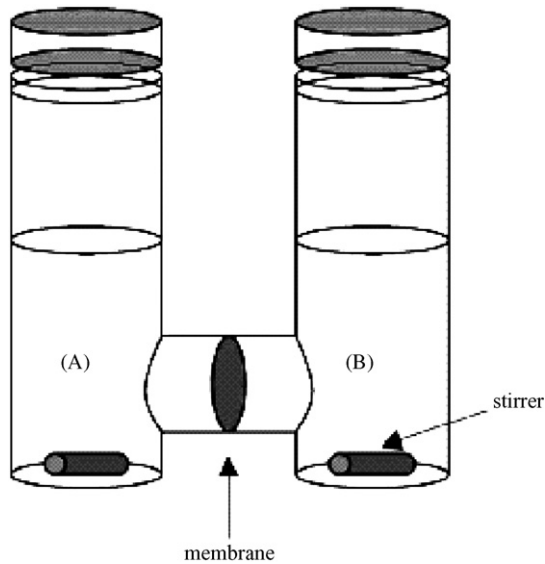


Fig. 1. Schematic representation of the methanol diffusion cell.

The proton conductivity was measured by ac impedance spectroscopy over a frequency range of  $10\text{--}10^7$  Hz with 50–500 mV oscillating voltage using an impedance/gain-phase analyzer (*Solatron 1260*) and an electrochemical interface (*Solatron 1287*). A sheet of composite membrane ( $30\text{ mm} \times 10\text{ mm}$ ) was placed in a test cell similar with previous reports [10,12] and this cell geometry was chosen to ensure that the membrane resistance dominated the response of the system [39]. The impedance measurements were performed in water with 100% relative humidity at desired temperature. Before measurement, the films were full hydrated in water for 24 h. The proton conductivity was calculated using the following equation:

$$\sigma = \frac{L}{RA} \quad (7)$$

where  $\sigma$  is the proton conductivity in  $\text{S cm}^{-1}$ ,  $L$  the distance between the two electrodes,  $R$  the ohmic resistance of the membrane and  $A$  is the cross-sectional area of membrane.

### 3. Result and discussion

#### 3.1. Characterization

FTIR and UV spectra were performed on the composite membranes to confirm the structures of the composite membranes. Fig. 2 shows the FTIR spectra of the SPEEK/TMBP composite membranes. The SPEEK membrane was confirmed by the characteristic absorption bands for asymmetric and symmetric O=S=O stretching vibrations of sulfonic acid groups at  $1274$ ,  $1079$  and  $1023\text{ cm}^{-1}$ , and the absorption band of the S–O stretching of sulfonic acid groups at  $685\text{ cm}^{-1}$ . In the spectra of SPEEK/TMBP, two of the bands were shifted to lower frequencies, i.e.  $1270$  and  $683\text{ cm}^{-1}$ . In the present case, sulfonic acid groups might have formed weak hydrogen bonds with amine functional groups [17,18]. Finally, a weak absorption band at  $1737\text{ cm}^{-1}$  was attributed to the C=O stretching of the amine. With the increment of TMBP, the intensity of the absorption

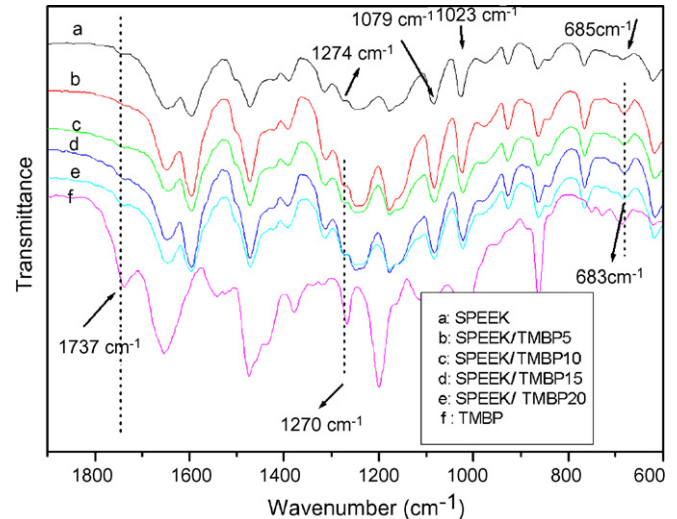


Fig. 2. FTIR spectra of SPEEK and SPEEK/TMBP composite membranes.

increased. It conformed to the trend of the weight ratio of TMBP in SPEEK membranes.

The UV spectra of the composite membranes are shown in Fig. 3. All the membranes showed absorption peaks at 210, 266 and 380–430 nm. The absorptions at 210 and 266 nm correspond to the stretching of the benzene. The absorption at 380–430 nm corresponded to the  $\pi\text{--}\pi^*$  transition of the benzenoid rings. The peaks shifted from 380 to 430 nm in the composite membranes, which may be due to the forming of interaction between the sulfonic acid groups and amine groups. The results of FTIR and UV spectra confirmed that the SPEEK/TMBP composite membranes have been successfully prepared.

#### 3.2. The morphology of the composite membranes

Atomic force microscopy (AFM) was performed to study the surface morphology of the composite membranes. As shown in Fig. 4, it can be seen that the surface of the SPEEK/TMBP composite membranes had become coarse and the number of 'particle' on the surface increased with the increment of TMBP

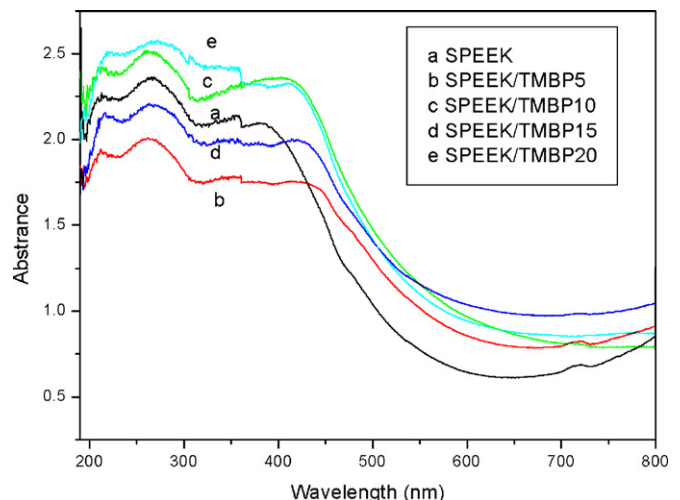


Fig. 3. UV curves of SPEEK and SPEEK/TMBP composite membranes.



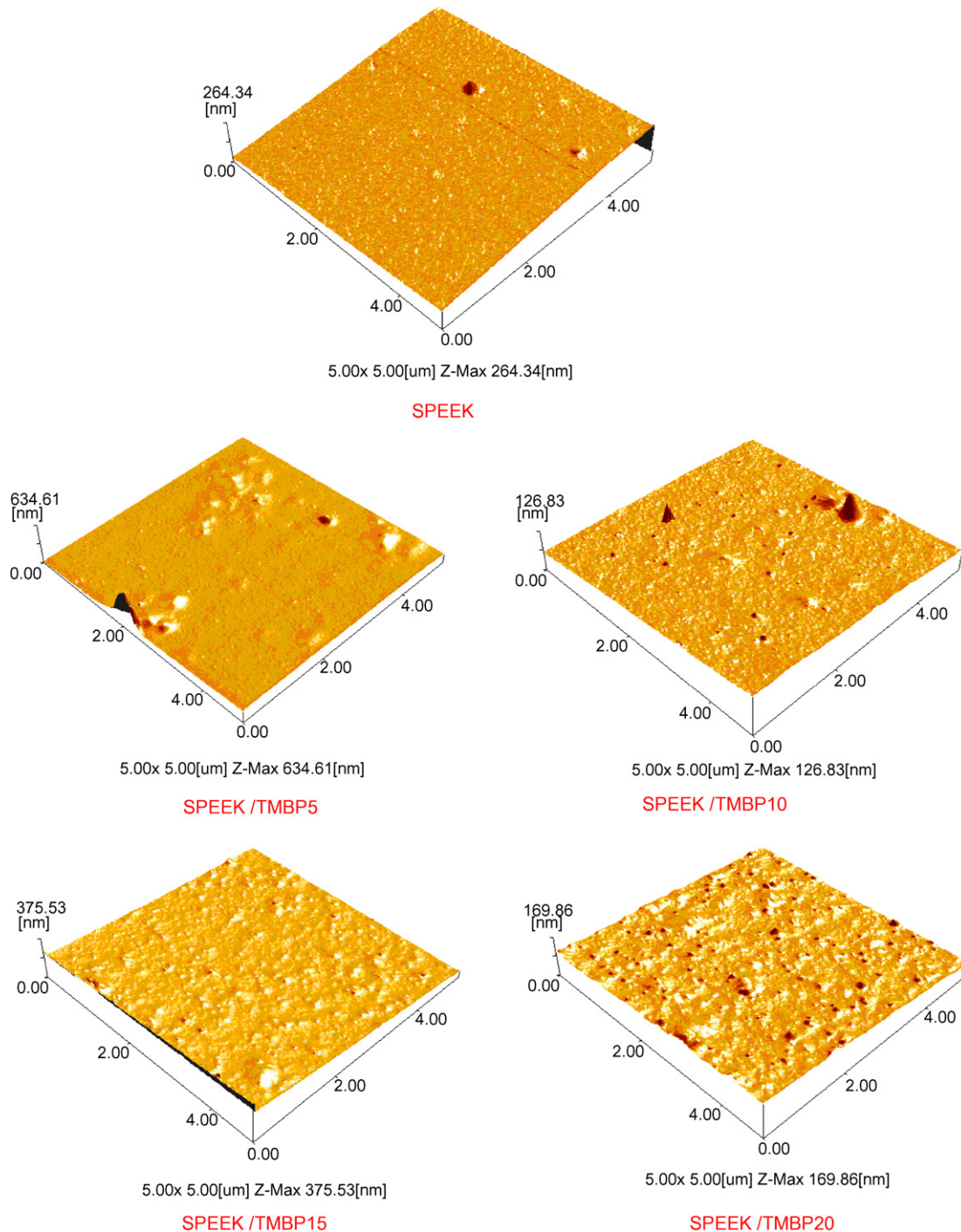


Fig. 4. The topographic image of SPEEK and SPEEK/TMBP composite membranes with different contents of TMBP.

and the size of it is about 20–50 nm. When the weight ratio of the TMBP is kept at 20%, the ‘particles’ were well distributed in the SPEEK matrix. This indicates that TMBP are homogeneously and well dispersed in the SPEEK membranes matrix.

### 3.3. The mechanical and thermal properties of the composite membranes

It is essential for PEMs to possess adequate mechanical strength. The typical mechanical properties of the compos-

ite membranes were evaluated and the results are listed in Table 1. The tensile modules for the membranes of SPEEK, SPEEK/TMBP5, SPEEK/TMBP10, SPEEK/TMBP15, and SPEEK/TMBP20 were 0.94, 1.04, 1.18, 1.24 and 1.26 GPa, respectively, and the tensile strengths were from 39 to 51 MPa. In the composite membrane, cured TMBP can form the three-dimensional network structure in SPEEK matrix, which can improve mechanical properties. The results indicated that the SPEEK/TMBP composite membranes were strong and tough enough for the

Table 1  
The mechanical properties of SPEEK and SPEEK/TMBP composite membranes

Composite membranes	Tensile strength (MPa)	Maximum elongation (%)	Tensile modulus (MPa)
SPEEK	39.75 ± 0.70	15.16 ± 3.81	945.70 ± 70.71
SPEEK/TMBP5	44.55 ± 1.32	9.56 ± 2.42	1041.67 ± 94.22
SPEEK/TMBP10	49.03 ± 1.80	8.78 ± 1.10	1186.90 ± 82.41
SPEEK/TMBP15	50.15 ± 1.06	12.14 ± 3.04	1241.14 ± 67.52
SPEEK/TMBP20	50.27 ± 0.43	7.87 ± 0.064	1259.27 ± 2.31

usages of functional proton exchange membrane (PEM) materials.

DSC and TGA measurements were carried out to testify the thermal properties of the composite membranes. The values of the glass transition temperatures ( $T_g$ ) from the DSC curves of the membranes are listed in Table 2. The DSC curves showed one thermal transition. The results confirmed that compatibility exists between SPEEK and TMBP and this may be ascribed to the presence of weak hydrogen bonds between the amide group of PA and sulfonic acid group of SPEEK. The  $T_g$  values of the composite membranes were all higher than 290 °C. The  $T_g$  value at 290 °C of the SPEEK/TMBP5 was the lowest. However, with the content of TMBP increased, the  $T_g$  values shifted to high temperature due to restrict the segmental motion of polymer chains. It may be mainly restricted due to the presence of cross-linking with occurrence of TMBP and PA. Thermal stabilities of SPEEK and SPEEK/TMBP composite membranes in acid forms were investigated by TGA as shown in Fig. 5 and the results are listed in Table 2. All membranes exhibited two distinct degradation steps. The first weight loss between 300 and 450 °C is closely attributed to the thermal degradation of sulfonic acid groups or main chains of TMBP. The second weight loss above 450 °C represents the thermal decomposition of the main chains of SPEEK and TMBP. Table 2 shows the onset weight loss temperatures ( $T_{onset}$ ) and 5% weight loss temperatures ( $T_{5\%}$ ) of SPEEK and SPEEK/TMBP composite membranes in acid forms are observed between 262–289 °C and 285–302 °C, respectively. The onset weight loss of composite membranes was closely associated with the thermal degradation of the flexible chains in PA. The TGA studies revealed good thermal properties of composite membranes for usage as proton conducting materials, which is also supported by DSC studies.

### 3.4. Water uptake, swelling ratio, water desorption of composite membranes

Water in the sulfonated polymers plays an important role in the proton exchange membrane and directly affects proton transport across their membranes [40]. Generally, it is believed

Table 2  
Thermal properties of SPEEK and SPEEK/TMBP composite membranes

Composites	SPEEK	SPEEK/TMBP5	SPEEK/TMBP10	SPEEK/TMBP15	SPEEK/TMBP20
$T_g$ (°C)	300	290	291	295	298
$T_{onset}$ (°C)	289	268	266	262	262
$T_{d5\%}$ (°C)	302	287	288	289	290

$T_{onset}$ , extrapolated onset for first weight loss;  $T_{d5\%}$ , temperature of 5% weight loss.

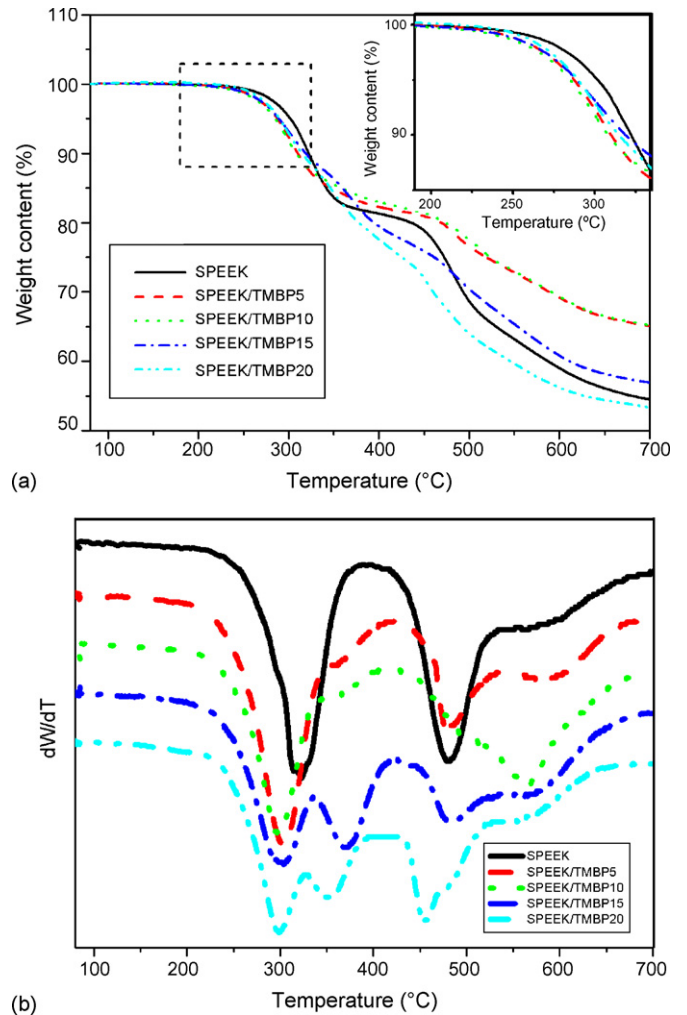


Fig. 5. The TGA (a) and derivative curves (b) for SPEEK and SPEEK/TMBP composite membranes.

Table 3  
The water uptake, swelling ratio, water desorption of SPEEK and SPEEK/TMBP composite membranes

Composite membranes	Water uptake (%)		Swelling ratio (%)		Water diffusion coefficient for desorption ( $\times 10^{-5} \text{ cm}^2 \text{ s}^{-1}$ )
	25 °C	80 °C	25 °C	80 °C	
SPEEK	31.31 $\pm$ 0.91	48.92 $\pm$ 1.10	22.37 $\pm$ 0.10	31.25 $\pm$ 0.12	8.82
SPEEK/TMBP5	28.83 $\pm$ 0.92	40.71 $\pm$ 1.02	10.00 $\pm$ 0.15	11.20 $\pm$ 0.20	2.58
SPEEK/TMBP10	22.54 $\pm$ 0.61	35.86 $\pm$ 0.73	8.52 $\pm$ 0.09	9.00 $\pm$ 0.17	1.82
SPEEK/TMBP15	17.38 $\pm$ 0.83	33.57 $\pm$ 0.71	7.54 $\pm$ 0.07	7.93 $\pm$ 0.09	0.98
SPEEK/TMBP20	13.85 $\pm$ 0.75	19.90 $\pm$ 0.90	3.17 $\pm$ 0.11	3.58 $\pm$ 0.13	0.87

that protons can be transported along with hydrogen-bonded ionic channels and cationic mixtures such as  $\text{H}_3\text{O}^+$ ,  $\text{H}_5\text{O}_2^+$ , and  $\text{H}_9\text{O}_4^+$  in the water [41]. The proton conductivity of membrane is very dependent on the connectivity of the hydrated domains. Therefore, the membrane must be able to absorb enough water. However, water uptake should be minimized to influence of the membrane mechanical and dimensional stability. So, it is very significant to determine the water uptake of the SPEEK/TMBP membrane for the PEM applications. To evaluate the water absorption and dimensional change, the water uptake values and swelling ratios of SPEEK and SPEEK/TMBP composite membranes in acid forms were measured from 25 to 80 °C, and the results are listed in Table 3. The water uptakes at different temperatures are shown in Fig. 6. Basically, the amount of water uptake in the sulfonated polymers will be strongly dependent upon the amount of sulfonic acid groups and will also be related to IEC values. It is well known that the cured epoxy resin with high cross-link density is hydrophobicity. When the content of hydrophobic TMBP increased, the content of the hydrophilic sulfonic functional groups fell, which were mainly responsible for the water uptake decreased. Therefore, the water uptake in the membrane decreased, the values of which were from 31.3% to 17.38% at 25 °C. The water uptake of membranes at 80 °C showed the similar tendency. The water uptake values of all of the composite membranes increased with the increasing of temperature, which corresponds to other articles [10–19]. Moreover, it

can be observed that an increase with introduction of hydrophobic TMBP in the SPEEK/TMBP membranes up to 20% leads to a substantial reduction in the swelling ratios of the composite membranes, the swelling ratio of the composite membranes showed a large scale decrease from 22.37% to 3.17% at room temperature and 31.25% to 3.58% at 80 °C, respectively. It indicated that the additional TMBP were necessary for dimensional stability in a fuel cell application.

Water retention of proton exchange membranes has significant effects on their proton conductivity, especially the water retention of membranes at high temperatures [41]. Nafion<sup>®</sup> with low water retention at high temperatures resulting in conductivity falls is one of the drawbacks, which limited their further commercial application. To investigate loosely bound water within composite membranes, water diffusion coefficients of composite membranes was analyzed by water desorption of hydrated membranes at 80 °C. The water desorption curves were shown in Fig. 7(a). The percent of weight loss of water decreased with the amount of sulfonic groups of the composite membranes indicating that the water molecules were strongly connected with hydrogen bonding around the sulfonic acid groups. This was consistent with the amount of water uptakes of membranes. Plots of  $M_t/M_\infty$  versus  $t_{1/2}$  initially are linear for Fickian diffusion laws [37] and are shown in Fig. 7(b). The water diffusion coefficients of the composite membranes calculated from the slope of the line are  $8.82 \times 10^{-5}$ ,  $2.58 \times 10^{-5}$ ,  $1.82 \times 10^{-5}$ ,  $0.98 \times 10^{-5}$ ,  $0.87 \times 10^{-5} \text{ cm}^2 \text{ s}^{-1}$ , respectively. As shown in results, the speed of diffusion of water decreased with the addition of TMBP. Hydrophobic TMBP networks hindered the water diffusion of membranes. That is to say that the water retention of the composite membranes at high temperatures is improved by the introduction of TMBP.

### 3.5. Ion-exchange capacity, methanol diffusion coefficient and proton conductivity

IEC is usually defined as the moles of fixed  $\text{SO}_3^-$  sites per gram of polymer. It plays a crucial role for the proton conductivity of the membranes in the fuel cell. Table 4 listed the titrated IEC values of the SPEEK and composite membranes. The titrated IEC values conformed to the content of fixed  $\text{SO}_3^-$  sites in the composite membranes. However, the number of water molecules per sulfonic site in Table 3 decreased with the content of TMBP up to 20% in composite membranes. This indicated the hydrogen bond between the sulfonic acid groups and amine groups have been formed as shown in FTIR.

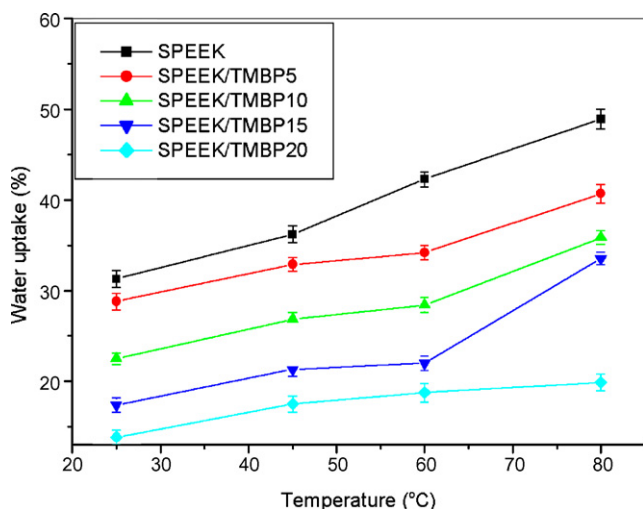


Fig. 6. Water uptakes of SPEEK and SPEEK/TMBP composite membrane at different temperatures.

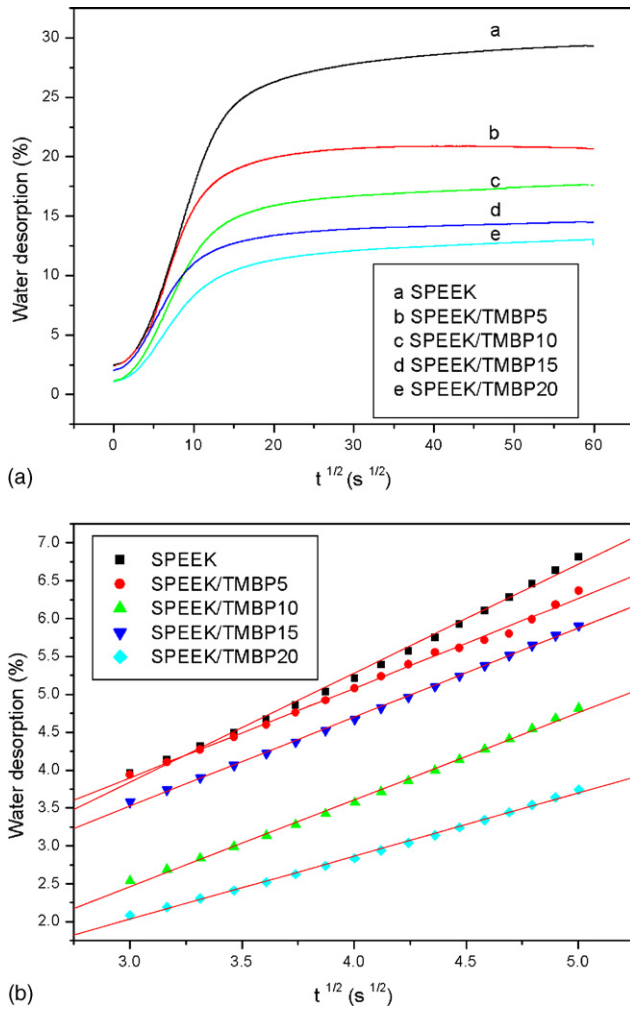


Fig. 7. Water desorption of SPEEK and SPEEK/TMBP composite membranes.

Methanol permeability and proton conductivity are the two transport properties, which both determine the fuel cell performance in DMFCs. Low methanol permeability and high proton conductivity are required for DMFCs. The transport of methanol among membrane also requires channels with good connectivity [42]. The content of well-connected channels decreased in composite membranes upon the introduction of TMBP, which is hydrophobic and have not sulfonic functional groups required for the formation of ion clusters and methanol transport channels. As shown in Table 3, the methanol permeability of the composite membranes decreased dramatically compared with the SPEEK membranes. The methanol permeability of SPEEK

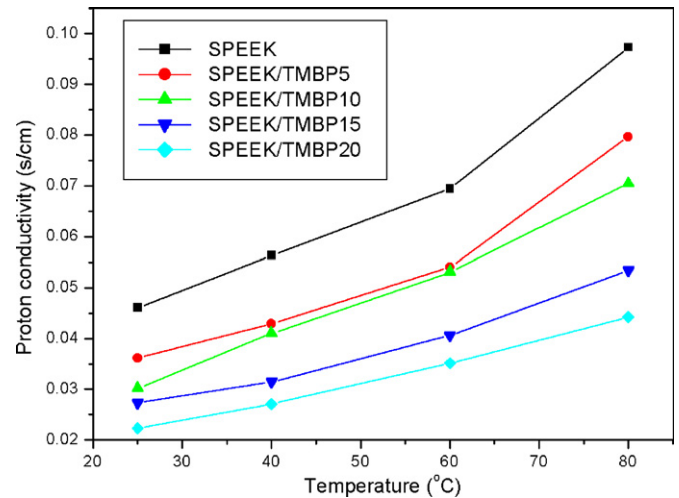


Fig. 8. Proton conductivity of SPEEK and SPEEK/TMBP composite membranes at different temperatures.

membranes is  $1.75 \times 10^{-6} \text{ cm}^2 \text{ s}^{-1}$  at room temperature, and that of the composite membranes is  $1.14 \times 10^{-6}$ ,  $8.04 \times 10^{-7}$ ,  $6.59 \times 10^{-7}$ ,  $5.26 \times 10^{-7} \text{ cm}^2 \text{ s}^{-1}$  with 5, 10, 15, 20 wt% of the TMBP, respectively.

The proton transport in membranes also requires well-connected channels formed by ion clusters of hydrophilic sulfonic functional groups. The content and the diameter of the connected channels have significant effects on the proton transport rate in membranes. When the density of sulfonic groups is low, the hydrophilic sulfonic groups form isolated ionic clusters in the continuous hydrophobic phase [41]. The diameter of the channels formed by ionic clusters may be also reduced upon the introduction of TMBP, which resulted from decrease of the density of sulfonic groups. As can be seen in Table 4, the proton conductivity of composite membranes decreased with the introduction of TMBP as resulted of the lower IEC, smaller water uptake, and poor ionic channel structure. The effect of temperature on the proton conductivity of the composite membranes is shown in Fig. 8. The proton conductivity is in general a thermally stimulated process. The proton conductivity of all of the composite membranes increased with the increasing of temperature. For examples, the proton conductivity of SPEEK membrane is  $0.046 \text{ S cm}^{-1}$  at  $25^\circ \text{C}$  and increases to  $0.097 \text{ S cm}^{-1}$  at  $80^\circ \text{C}$ . All composite membranes showed good proton conductivity more than  $10^{-2} \text{ S cm}^{-1}$ , which is the lowest value of practical interest for use as PEMs in fuel cells. Here, the selectivity means the characteristic factor for evaluating membrane performances

Table 4  
The properties of SPEEK and SPEEK/TMBP composite membranes

Composite membranes	IEC ( $\text{mmol g}^{-1}$ )	$\lambda$ ( $\text{H}_2\text{O}/\text{SO}_3^{-1}$ )	Methanol diffusion ( $\times 10^{-7} \text{ cm}^2 \text{ s}^{-1}$ )	Proton conductivity ( $\text{S cm}^{-1}$ )	
				$25^\circ \text{C}$	$80^\circ \text{C}$
SPEEK	$1.772 \pm 0.051$	9.82	17.5	0.046	0.097
SPEEK/TMBP5	$1.697 \pm 0.045$	9.44	11.4	0.036	0.080
SPEEK/TMBP10	$1.542 \pm 0.067$	8.12	8.04	0.030	0.070
SPEEK/TMBP15	$1.376 \pm 0.058$	7.02	6.59	0.027	0.053
SPEEK/TMBP20	$1.178 \pm 0.087$	6.53	5.26	0.022	0.044



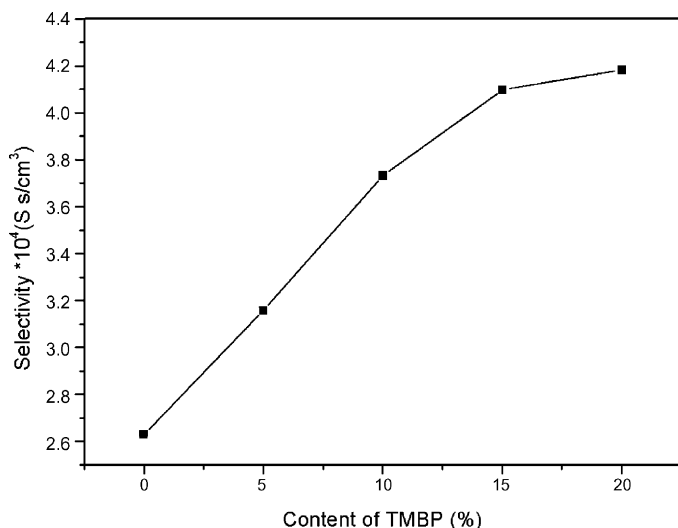


Fig. 9. Selectivity values ( $\sigma/DK$ ) of SPEEK and SPEEK/TMBP composite membranes.

considering both proton conductivity and methanol permeability. In this case, the selectivity can be used just as a barometer to develop the best proton conductive polymer membranes with reduced methanol permeability. Fig. 9 shows the selectivity defined as the ration of proton conductivity to methanol permeability of SPEEK and SPEEK/TMBP composite membranes. Though proton conductivities of the SPEEK/TMBP membranes were lower than those of SPEEK membrane, higher selectivity values were found for SPEEK/TMBP membranes in comparison with SPEEK membranes. The result suggests that the incorporation of TMBP into the SPEEK membranes had more impact on the reduction of methanol permeability than proton conductivity, and the composite membranes are attractive for DMFCs.

#### 4. Conclusion

The SPEEK/TMBP composite membranes have been prepared by *in situ* polymerization method. The mechanical properties of SPEEK membrane was improved with the introduction of TMBP. However, the thermal stabilities of SPEEK/TMBP membranes were slightly decreased with the introduction of TMBP. The water uptake and the swelling ratio of SPEEK/TMBP membranes were reduced rapidly. When the content of TMBP up to 20%, the water uptake and swelling ratio have been decreased to 13.85% and 3.17%, respectively. The water retention of the composite membranes at high temperatures was improved. Though proton conductivities of the SPEEK/TMBP membranes were lower than those of SPEEK membrane, higher selectivity values defined as the ratio of proton conductivity to methanol permeability were found for SPEEK/TMBP membranes in comparison with SPEEK membranes. The SPEEK/TMBP composite membranes show good potential for the usage in DMFCs.

#### References

- [1] J.P. Shoesmith, R.D. Collins, M.J. Oakley, D.K. Stevenson, J. Power Sources 49 (1994) 129.
- [2] S. Gamburgzev, A.J. Appleby, J. Power Sources 107 (2002) 5.
- [3] A.J. Appleby, Phys. Eng. Sci. 354 (1996) 1681.
- [4] B.C. Johnson, I.C. Yilgor, T.M. Iqbal, J.P. Wightmen, J. Polym. Sci. 22 (1984) 721.
- [5] J.J. Dumais, A.L. Cholli, L.W. Jelinski, J.E. McGrath, Macromolecules 19 (1986) 1884.
- [6] Y.S. Kim, L. Dong, M.A. Hickner, B.S. Pivovar, J.E. McGrath, Polymer 44 (2002) 5729.
- [7] F. Wang, M.A. Hickner, Q. Ji, W.L. Harrison, J.F. Mechem, T.A. Zawodzinski, J.E. McGrath, Macromol. Symp. 175 (2001) 387.
- [8] X.F. Li, Z. Wang, H. Lu, C.J. Zhao, H. Na, J. Membr. Sci. 254 (2005) 147.
- [9] X.F. Li, C.J. Zhao, H. Lu, Z. Wang, H. Na, Polymer 46 (2005) 5820.
- [10] X.F. Li, C.P. Liu, H. Lu, C.J. Zhao, Z. Wang, H. Na, J. Membr. Sci. 255 (2005) 149.
- [11] C. Manea, M. Mulder, Desalination 147 (2002) 179.
- [12] M. Gil, X.L. Ji, X.F. Li, H. Na, J.E. Hampsey, Y.F. Lu, J. Membr. Sci. 234 (2004) 75.
- [13] F. Wang, T.L. Chen, J.P. Xu, Macromol. Chem. Phys. 199 (7) (1998) 1421.
- [14] S.D. Mikhailenko, S.M. Zaidi, S. Kaliaguine, Catal. Today 67 (2001) 225.
- [15] S.D. Mikhailenko, K.P. Wang, S. Kaliaguine, P.X. Xing, et al., J. Membr. Sci. 233 (2004) 93.
- [16] X.F. Li, H. Na, H. Lu, J. Appl. Polym. Sci. 94 (2004) 1569.
- [17] W. Cui, J. Kerres, G. Eigenberger, Sep. Purif. Technol. 14 (1998) 145.
- [18] J. Kerres, A. Ullrich, F. Meier, T. Haring, Solid State Ionics 125 (1–4) (1999) 243.
- [19] W. Jang, S. Sundar, S. Choi, Y.G. Shul, H. Han, J. Membr. Sci. 280 (1–2) (2006) 321.
- [20] X.F. Li, D.J. Chen, D. Xu, C.J. Zhao, Z. Wang, H. Lu, H. Na, J. Membr. Sci. 275 (2006) 134.
- [21] X.F. Li, C.P. Liu, D. Xu, C.J. Zhao, Z. Wang, G. Zhang, H. Na, W. Xing, J. Power Sources 162 (2006) 1.
- [22] J. Gu, S.C. Narang, E.M. Pearce, J. Appl. Polym. Sci. 30 (1985) 2997.
- [23] R.J. Norgan, E.T. Mones, W.J. Steele, Polymer 23 (1982) 295.
- [24] J.Y. Lee, M.J. Shim, S.W. Kim, Mater. Chem. Phys. 48 (1997) 36.
- [25] J.Y. Lee, M.J. Shim, S.W. Kim, J. Appl. Polym. Sci. 81 (2001) 479.
- [26] C.L. Carfagna, E. Amendola, M. Giamberini, A. Filippov, R.S. Bauer, Liq. Cryst. 13 (1993) 571.
- [27] M. Ochi, N. Tsuyuno, K. Sakaga, Y. Nakanishi, Y. Murata, J. Appl. Polym. Sci. 56 (1995) 1161.
- [28] W. Mormann, M. Brocher, Macromol. Chem. Phys. 197 (1996) 1841.
- [29] W.F.A. Su, J. Polym. Sci. Pt. A: Polym. Chem. 31 (1993) 3251.
- [30] W.F.A. Su, K.F. Schoch, J.D.B. Smith, J. Appl. Polym. Sci. 70 (1998) 2163.
- [31] W.F.A. Su, H.W. Huang, W.P. Pan, Thermochim. Acta 392/393 (2002) 391.
- [32] W.F.A. Su, Y.C. Lee, W.P. Pan, Thermochim. Acta 392/393 (2002) 395.
- [33] C.L. Zhang, H. Na, C.G. Liu, Thermosetting Resin 17 (1) (2002) 1.
- [34] C.L. Zhang, H. Na, J.X. Mu, Chem. J. Chinese U. 25 (9) (2004) 1756.
- [35] C.L. Zhang, J.X. Mu, W.Z. Yu, Chem. J. Chinese U. 25 (10) (2004) 1937.
- [36] Y.Z. Fu, A. Manthiram, J. Power Sources 157 (2006) 222.
- [37] T. Watari, H.Y. Wang, K. Kuwahara, K. Tanaka, H. Kita, K. Okamoto, J. Membr. Sci. 219 (2003) 137.
- [38] B. Jung, B.Y. Kim, J.M. Yang, J. Membr. Sci. 245 (2004) 61.
- [39] F. Wang, M.S. Hickner, Y.S. Kim, T.A. Zawodzinski, J.E. McGrath, J. Membr. Sci. 197 (2002) 231.
- [40] T.A. Zawodzinski, J. Davey, J. Valerio, S. Gottesfeld, Electrochim. Acta 40 (1995) 297.
- [41] A.A. Kornshev, A.M. Kuznetsov, E. Spohr, J. Ulstrup, J. Phys. Chem. B 107 (2003) 3351.
- [42] S. Xue, G.P. Yin, Polymer 47 (2006) 5044.